In-plane and Out-of-plane Motion of Benzene Trapped in a Cd(py)$_2$\{Ag(CN)$_2$\}$_2$ Host as Studied by Deuterium NMR

SHIN-ICHI NISHIKIORI,* TAKAYOSHI SOMA and
TOSCHITAKE IWAMOTO
Department of Basic Science, Graduate School of Arts and Sciences, The University of Tokyo, 3-8-1 Komaba, Meguro-ku, Tokyo 153, Japan

Abstract. ^{2}H-NMR powder patterns of the deuterated benzene molecule trapped in a Cd(py)$_2$\{Ag(CN)$_2$\}$_2$ host were measured in the temperature range of 123–403 K in order to obtain information about motional behavior of the guest benzene molecule undergoing an in-plane motion combined with an out-of-plane motion. The activation energy for the in-plane motion, which is a 60° jump among neighboring sites on the benzene ring, was derived to be 18.2(5) kJ mol^{-1} from the line-shape simulation of the ^{2}H-NMR powder patterns. The jump frequency of the out-of-plane motion, which is a reorientation of the benzene ring between two sites separated with a 57.8^o azimuthal angle, was in a fast motion region even at 123 K and the activation energy of the two-site jump is very low compared with that of the in-plane motion.

Key words: Metal cyanide, benzene clathrate compound, ^{2}H-NMR, molecular motion

1. Introduction

Host–guest systems having a variety of host structure types are currently being designed and developed. The motional behavior of a guest molecule trapped in a host attracts the attention of chemists interested in evaluating the cavity structure and the host-guest interaction of such hosts. Perhaps one of the most popular guest molecules is benzene, and information on the motional behavior of a guest benzene molecule is a starting point for considering the motional behavior of other guest molecules. Several investigations of the motion of a guest benzene molecule have already been conducted. In many cases the guest benzene molecule undergoes an in-plane reorientation about its six-fold axis, and motion of this kind has been well analyzed [1–5]. However, the following idea is likely: if a guest benzene molecule has a spatial freedom toward its out-of-plane directions in a cavity, an out-of-plane reorientational motion with small amplitude can easily occur, compared with an in-plane motion. It is not easy to confirm the above idea experimentally, because it is difficult to obtain structural support from the X-ray structure determination due to disorder and/or large displacement parameters of the

---

* Author for correspondence.

guest molecule under such conditions. And this situation makes it difficult to make an appropriate model of a guest molecular motion for analyzing NMR data. There are a few investigations in which an analysis including an out-of-plane motion has been done [5, 6]. However, information on the out-of-plane motion is still scarce. In this study, we investigated benzene's in-plane motion combined with an out-of-plane motion by applying the ^{2}H-NMR technique to a benzene clathrate compound in order to obtain information about any correlation between the two motions. We chose a $Cd(py)_2\{Ag(CN)_2\}_2$ benzene clathrate compound as a target (py = pyridine) [7]. Figure 1 shows the crystal structure of the clathrate. The host of the clathrate has an interpenetrating structure of two-dimensional $[Cd(py)_2\{Ag(CN)_2\}_2]$ complex networks which are built of long, linear —NC—Ag—CN— bridges [7]. A single crystal X-ray diffraction experiment at room temperature revealed that the guest benzene molecule was in a disordered state, with two benzene molecules being diagonally overlapped, as shown in Figure 2. The following four cases are possible for the state of the benzene molecule: (1) a static state, (2) an in-plane 6-site motion with no out-of-plane motion, (3) an out-of-plane motion with no in-plane motion, and (4) an in-plane 6-site motion combined with an out-of-plane motion. Solid state ^{2}H-NMR is a useful method for revealing the state of the guest benzene molecule. In the case of state (4), it is possible to obtain information of each motion from analysis of ^{2}H-NMR data.

2. Experimental

2.1. PREPARATION

The sample used in ^{2}H-NMR measurement was prepared by the method described in our previous report [7]. Deuterated benzene (C_6D_6 99.5%D, purchased from Merck) was used instead of normal benzene. Colorless crystals of $Cd(py)_2\{Ag(CN)_2\}_2 \cdot C_6D_6$ were obtained after leaving the mother solution in a refrigerator for a week.

2.2. ^{2}H-NMR MEASUREMENT

A Chemagnetics CMX300 spectrometer fitted with a nitrogen gas flow temperature controller was used in the ^{2}H-NMR powder pattern measurement. The measurement was carried out at 46.6 M Hz Larmor frequency in the temperature range of 123–413 K using the quadrupole echo pulse sequence [8, 9] of 2 μs 90° pulse, 35 μs spacing time and 1–10 s recycle delay. Figures 3(a)–3(l) show the patterns observed at different temperatures.

2.3. LINE-SHAPE SIMULATION OF ^{2}H-NMR SPECTRA

The method of simulating ^{2}H-NMR powder patterns based on a motional model had been established by several experts [10–13]. The line-shape simulation in this
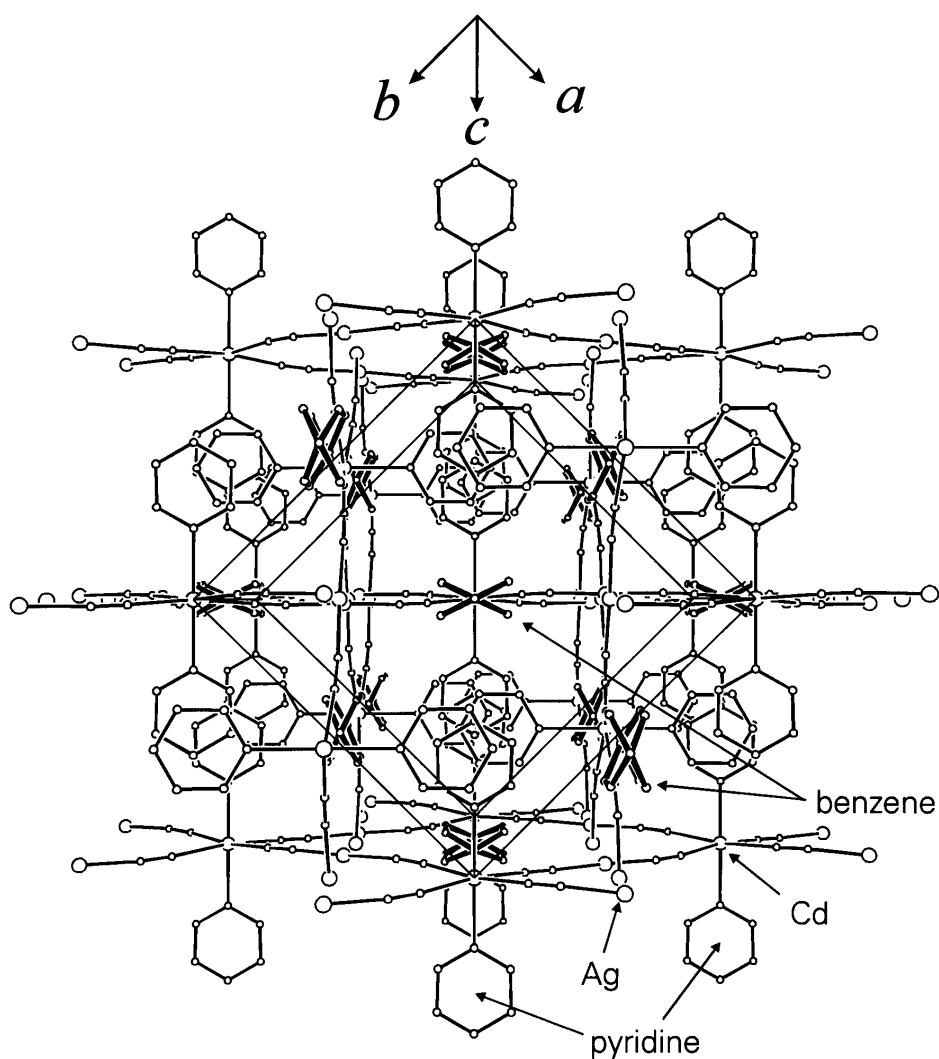
Figure 1. A perspective view of $Cd(py)_2\{Ag(CN)_2\}_2 \cdot C_6H_6$ along the c axis [7].

study was performed using a FORTRAN program written by the authors based on the calculation principle described by Vega and Luz [11] (see Appendix). Values of the quadrupole coupling constant (Qcc) and the asymmetry parameter (η) for static benzene, 183 kHz and 0.04, that were necessary in the simulation, were taken from the work of Ok et al. [5]. Because the powder pattern observed at 123 K, which is the lowest controllable temperature of our NMR instruments, did not show a pattern in a static state (Figure 3(a)), we could not determine both values. The above values were obtained from ^{2}H-NMR powder pattern measurement of neat deuterated benzene at 87 K [5]. The calculation was performed on an IBM
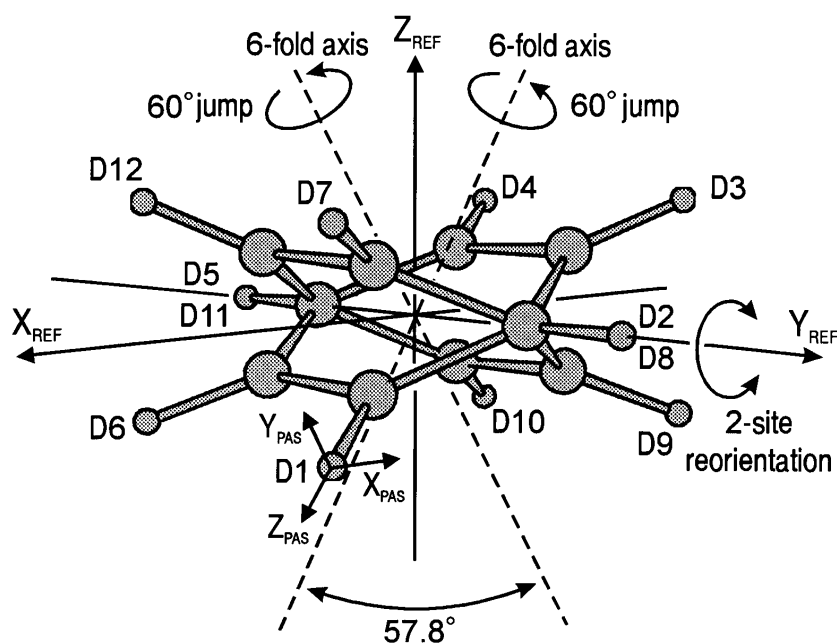
Figure 2. The disordered guest benzene molecule in a Cd(py)$_2$ {Ag(CN)$_2$}$_2$ host and a reference frame (REF) for prescribing a motional model. REF is indicated with the X_{REF}, Y_{REF}, Z_{REF} axes. The in-plane motion combined with an out-of-plane motion model is described as the combination of an in-plane 6-site reorientation which is a 60° jump about the 6-fold axis and an out-of-plane reorientation of the benzene ring between two sites separated with 57.8° azimuthal angle about the Y_{REF} axis. The principal axis system (PAS) of the electric field gradient of the deuterium at site 1 is indicated with the X_{PAS}, Y_{PAS}, Z_{PAS} axes.

SP2 computer of the Computer Center, Institute for Molecular Science, Okazaki National Research Institutes. Figures 3(m)–3(v) show best fit results.

3. Results and Discussion

Based on the results of the X-ray diffraction study, we listed four possible cases for the state of the guest benzene molecule in the Introduction. The observed temperature dependence of the powder patterns in Figure 3(a)–3(l) shows that the guest molecule is not in a static state but a motional state. The powder pattern observed at 294 K (Figure 3(j)) formed the beginning of our line shape analysis. No change was observed in the shape and intensity of the pattern at 294 K when measured with a spacing time of 70 μs instead of 35 μs. This finding indicates that the pattern is in a fast limit region of the NMR time scale. In a fast limit case, it is not too difficult to analyze how many deuteriums in different motional modes give rise to a powder pattern. Judging from the line shape, the pattern at 294 K originates with one kind of deuterium. In other words, the guest benzene molecule is undergoing a motion that averages all the six deuteriums of the benzene molecule. As the
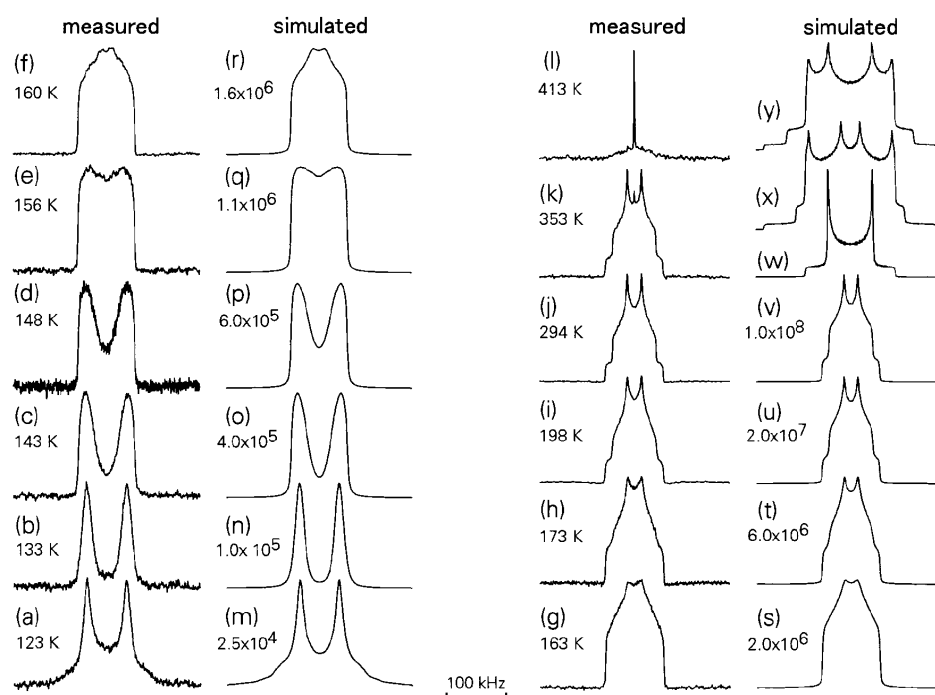
Figure 3. (a)–(l) : observed ^{2}H-NMR powder patterns. (m)–(v): powder patterns simulated on the basis of the model of the in-plane 6-site reorientation combined with the out-of-plane 2-site reorientation. Jump frequencies of the in-plane reorientation (k_i/s^{-1}) are indicated in the figure. Jump frequency of the out-of-plane reorientation (k_0) was fixed at $1 \times 10^8 \, s^{-1}$. (w): a simulated powder pattern of the simple in-plane 6-site reorientation. (x): a simulated powder pattern of the 180° flipping motion. (y): a simulated powder pattern of the out-of-plane 2-site reorientation about the Y_{REF} axis in Figure 2, where the separate angle between the two sites was assumed to be 57.8°. Each jump frequency used in the calculations of (w), (x) and (y) was $1 \times 10^8 \, s^{-1}$. In all simulations line broadening was applied using a Lorentzian broadening function with a half width of 1 kHz.

second case (see the Introduction), we considered an in-plane 6-site reorientation, which is a 60° jump among adjacent sites on the same benzene ring. This motion averages all the six deuteriums of the benzene molecule. However, the in-plane 6-site reorientation was considered not to be the guest molecular motion. The calculated powder pattern based on the in-plane 6-site reorientation model, the line shape of which is shown in Figure 3(w), did not coincide with the pattern at 294 K. Two models were considered for the third case in the Introduction, viz., an out-of-plane motion with no in-plane motion. One is a 180° flipping of the benzene ring about the Y_{REF} axis in Figure 2, and another is a reorientation of the benzene ring between two sites about the Y_{REF} axis in Figure 2. These motions generate two kinds of deuterium in different motional modes. Therefore, their powder patterns have complicated line shapes as shown in Figures 3(x) and 3(y), and these motional models were discarded.

We now present a model of the fourth case: the benzene is undergoing in-plane 6-site reorientation and at the same time the benzene ring is undergoing out-of-plane two-site reorientation about the Y_{REF} axis, as illustrated in Figure 2. If the separation angle between the two sites is assumed to be $57.8°$, the powder pattern at 294 K is reproduced with discrepancy of a few kHz line width, as shown in Figures 3(j) and 3(v). The dihedral angle between two least-squares planes of the two disordered benzene rings was calculated to be $54(2)°$ from the X-ray structure data.

From the viewpoint of the crystal structure, another motional model is possible as the fourth case: an in-plane 6-site reorientation and a $180°$ flipping of the benzene ring about the Y_{REF} axis taking place at the same time. However, we discarded this model. Because the $180°$ flipping gives no effect to the electric field gradient which is averaged by the in-plane 6-site reorientation, the powder pattern of this combined motion is equivalent to that of the simple in-plane 6-site reorientation (Figure 3(w)).

Above 294 K, a sharp line appeared at the center of the powder pattern (Figure 3(k)), and by 413 K the powder pattern disappeared and the sharp line became the main one (Figure 3(l)). This change of the line shape comes from thermal decomposition of the host lattice. Thermogravimetry showed that loss of the guest benzene and the pyridine, which is a part of the host lattice, commenced from about 350 K, and the benzene and the pyridine were completely lost in a one-step reaction by 453 K. It is therefore considered that the central sharp peak comes from the random motion of the benzene guest escaping from the damaged host lattice. After warming up to 413 K the sample showed no NMR signal.

The change of shape and intensity of the powder patterns was observed in the temperature range from 123 K to 198 K. This change indicates that the rate of the motion is in an intermediate region of the NMR time scale. The simulation of these patterns was carried out by varying each jump frequency of the two motions in the motional model of the in-plane 6-site reorientation combined with the out-of-plane 2-site reorientation. Each jump frequency was scanned from 1×10^3 s^{-1} to 1×10^8 s^{-1}, independently. The best fit results are displayed in Figures 3(m)–3(v). The patterns were well simulated under the conditions that the jump frequency of the out-of-plane reorientation (k_0) was fixed at 1×10^8 s^{-1} and that of the in-plane reorientation (k_i) was varied between 2.5×10^4 s^{-1} and 1×10^8 s^{-1}. This finding indicates that the out-of-plane reorientational frequency is very high, in the sense of the NMR time scale, even at 123 K, and the activation energy for the out-of-plane motion is too low to be determined from our measurement. On the other hand, the activation energy for the in-plane motion was derived to be 18.2(5) k J mol^{-1} from an Arrhenius plot of jump frequency k_i vs $1/T$, shown in Figure 4. Literature values for the activation energy of the in-plane reorientation of a benzene molecule in a solid are found in the range from 7–25 kJ mol^{-1} [5, 14]. Our value, 18.2(5) kJ mol^{-1}, is considered to be a common one for this type of motion.

In the Cd(py)$_2${Ag(CN)$_2$}$_2$·C$_6$D$_6$ clathrate compound, we have confirmed that the activation energy of the out-of-plane reorientation is lower than that of the in-
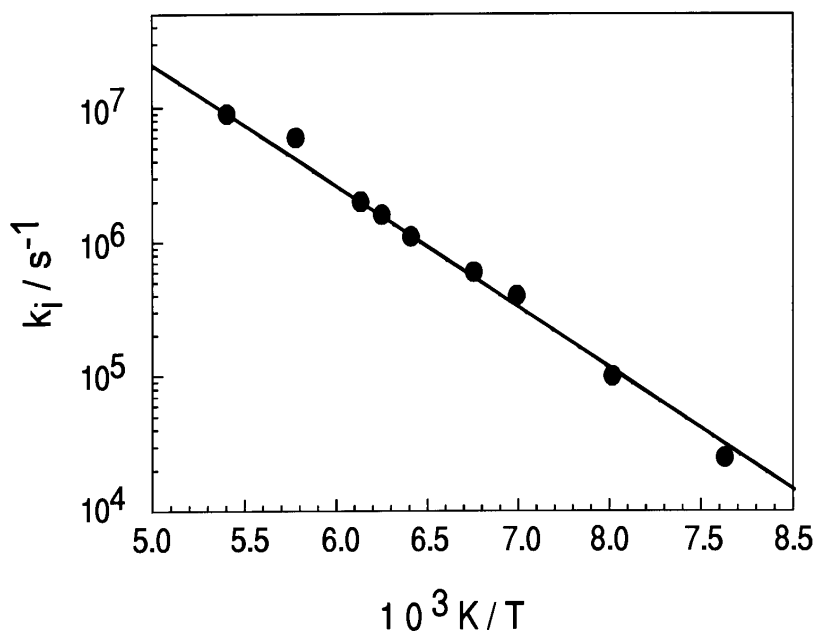
Figure 4. An Arrhenius plot of the jump frequencies for the in-plane 6-site reorientation (k_i) vs. $1/T$. The activation energy of the in-plane 6-site reorientation was derived to be 18.2(5) kJ mol^{-1} from the slope of the plot.

plane reorientation by using a simulation that explicitly includes the jump frequencies of both motions. However, there are a few studies reporting that the activation energy of an out-of-plane motion becomes higher than that of an in-plane motion [6, 15]. In such cases, a benzene molecule is in an out-of-plane motion with larger reorientational amplitude such as a 180° flipping, an n-site reorientation $(n \geq 3)$ and a rotation about a 2-fold axis on its benzene ring. It is reasonable that a motion with larger amplitude has a higher activation energy. We now need to investigate and clarify the boundary between the above two contrary cases. However, data on an in-plane motion combined with an out-of-plane motion are inadequate at the present time. More structural and motional data of other examples are needed to discuss this type of guest molecular motion in general.

Appendix

CALCULATION METHOD OF A ²H-NMR POWDER PATTERN

The basic principle of the ²H-NMR powder pattern simulation is to describe the behavior of an effective complex magnetization $\overrightarrow{\mathbf{G}}$ on a Larmor frequency rotat-

ing frame using a Bloch-type equation (Equation 1) along the quadrupole pulse sequence [11–13].

$$\frac{d\overrightarrow{\mathbf{G}}}{dt} = \mathbf{R}\overrightarrow{\mathbf{G}}(t). \tag{1}$$

The echo signal after time t from the starting point of the data acquisition is

$$E(t) = \mathrm{Re}\{\overrightarrow{\mathbf{1}}\exp(\mathbf{R}t)\exp(\mathbf{R}\tau)\exp(\mathbf{R}\tau)^{*}\overrightarrow{\mathbf{P}}\}$$

where τ is the spacing time of the quadrupole pulse sequence, $\overrightarrow{\mathbf{P}}$ is a vector of population (p_j) for each deuterium site and $\overrightarrow{\mathbf{1}}$ is a vector of unit elements for summing matrix elements. Spectrum $I(w)$ is obtained from Fourier transformation of the echo signal,

$$I(w) = \int_{0}^{\infty} E(t)\cos wt\, dt.$$

A powder pattern $J(w)$ is obtained by integrating $I(w)$ over all directions,

$$J(w) = \frac{1}{8\pi^2}\int_{0}^{2\pi}\int_{0}^{\pi} I(w)\sin\beta_2\, d\beta_2\, d\gamma_2$$

where β_2 and γ_2 are Euler angles for describing the direction of a reference frame in a laboratory frame (see below).

In the Bloch-type equation (Equation 1), $\mathbf{R}$ is a rate matrix,

$$\mathbf{R} = \mathbf{K} + \mathbf{B} + i\mathbf{W}. \tag{2}$$

Matrix $\mathbf{K}$ is a jump matrix which defines frequencies of jumps in a motional model. A non-diagonal element k_{ij} is defined as a frequency [sec^{-1}] of the jump from site j to site i, where a relation of $p_i k_{ji} = p_j k_{ij}$ holds. A diagonal element k_{ii} is described as $k_{ii} = -\sum_{i \neq j} k_{ji}$. Namely, $-1/k_{ii}$ is the lifetime at site i caused by a molecular motion.

Matrix $\mathbf{B}$ is a diagonal matrix of $-1/T_2$ for a line broadening effect caused by inhomogeneous magnetic fields. Using matrix $\mathbf{B}$, a theoretical line shape is convoluted with a Lorentzian broadening function with a full width at half maximum of $1/\pi T_2$. In our program, it is assumed that each site has a common T_2.

Matrix $\mathbf{W}$ is a diagonal matrix of the shift from the Larmor frequency at each deuterium site. A procedure for calculating the shift is shown below. The Hamiltonian of the electric quadrupole is described as

$$\widehat{H}_Q = \frac{eQ}{2I(2I-1)}\widehat{\overrightarrow{\mathbf{I}}}_{\mathrm{PAS}}\mathbf{V}_{\mathrm{PAS}}\widehat{\overrightarrow{\mathbf{I}}}_{\mathrm{PAS}} \tag{3}$$

in a principal axis system of the electric field gradient. $\mathbf{V}_{\text{PAS}}$ is the electric field gradient tensor,

$$\mathbf{V}_{\text{PAS}} = \frac{-eq}{2} \begin{pmatrix} V_{xx} & 0 & 0 \\ 0 & V_{yy} & 0 \\ 0 & 0 & V_{zz} \end{pmatrix}$$

where $V_{xx} = 1 - \eta$, $V_{yy} = 1 + \eta$, $V_{zz} = -2$ and η is the asymmetry factor $(0 \leq \eta \leq 1)$. The z direction of $\mathbf{V}_{\text{PAS}}$ coincides with the direction of a C—D bond axis. In order to carry out the calculation on a laboratory frame (LAB) the z axis of which is parallel to the direction of the external magnetic field, we consider two coordinate transformations. One ($\mathbf{T}_1$) is for rotating a molecule-fixed reference frame (REF), which is fixed for prescribing a molecular motion, into a principal axis system (PAS) of the electric field gradient at a deuterium site. Another ($\mathbf{T}_2$) is for rotating LAB into REF in order to perform an integral over all directions for making a powder pattern. $\mathbf{T}_i$ is defined as in Equation 4 using the Euler angles $(\alpha_i, \beta_i, \gamma_i)$.

$$\mathbf{T}_i(\alpha_i, \beta_i, \gamma_i) = \begin{pmatrix} \cos\gamma_i & \sin\gamma_i & 0 \\ -\sin\gamma_i & \cos\gamma_i & 0 \\ 0 & 0 & 1 \end{pmatrix} \begin{pmatrix} \cos\beta_i & 0 & -\sin\beta_i \\ 0 & 1 & 0 \\ \sin\beta_i & 0 & \cos\beta_i \end{pmatrix}$$
$$\times \begin{pmatrix} \cos\alpha_i & \sin\alpha_i & 0 \\ -\sin\alpha_i & \cos\alpha_i & 0 \\ 0 & 0 & 1 \end{pmatrix}. \tag{4}$$

The electric field gradient tensor described in LAB is

$$\mathbf{V}_{\text{LAB}} = {}^t\mathbf{T}_2 \, {}^t\mathbf{T}_1 \mathbf{V}_{\text{PAS}} \mathbf{T}_1 \mathbf{T}_2,$$

and Equation 3 becomes

$$\widehat{H}_Q = \frac{eQ}{2I(2I-1)} \overset{\frown}{\mathbf{I}}_{\text{LAB}} \mathbf{V}_{\text{LAB}} \overset{\frown}{\mathbf{I}}_{\text{LAB}}. \tag{5}$$

Neglecting the non-secular part of Equation 5, we obtain

$$\widehat{H}_Q = \frac{-e^2 Qq}{8} V'_{\text{LAB}_{33}}(3\widehat{I}_Z^2 - 2)$$

where $V'_{\text{LAB}_{33}}$ is the 3–3 element of $(-2/eq)\mathbf{V}_{\text{LAB}}$. And the shift from the Larmor frequency for site j in angular frequency units is described as:

$$w_j = \frac{-3\pi}{4} Qcc V'_j$$

where Qcc is the quadrupole coupling constant, and

$$
\begin{aligned}
V_j' = {} & \cos\beta_2(C_{24}\cos\beta_2 - C_{21}\cos\gamma_2\sin\beta_2 + C_{22}\sin\beta_2\sin\gamma_2) \\
& - \cos\gamma_2\sin\beta_2(C_{21}\cos\beta_2 - C_{25}\cos\gamma_2\sin\beta_2 + C_{23}\sin\beta_2\sin\gamma_2) \\
& + \sin\beta_2\sin\gamma_2(C_{22}\cos\beta_2 - C_{23}\cos\gamma_2\sin\beta_2 + C_{26}\sin\beta_2\sin\gamma_2)
\end{aligned}
$$

$C_1 = \cos\gamma_{1j}\sin\beta_{1j}$
$C_2 = \sin\beta_{1j}\sin\gamma_{1j}$
$C_3 = -2\cos\alpha_{1j}\cos\beta_{1j}\sin\beta_{1j}$
$C_4 = -\cos\gamma_{1j}\sin\alpha_{1j} - \cos\alpha_{1j}\cos\beta_{1j}\sin\gamma_{1j}$
$C_5 = \cos\alpha_{1j}\cos\beta_{1j}\cos\gamma_{1j} - \sin\alpha_{1j}\sin\gamma_{1j}$
$C_6 = -2\cos\beta_{1j}\sin\alpha_{1j}\sin\beta_{1j}$
$C_7 = \cos\beta_{1j}\cos\gamma_{1j}\sin\alpha_{1j} + \cos\alpha_{1j}\sin\gamma_{1j}$
$C_8 = \cos\alpha_{1j}\cos\gamma_{1j} - \cos\beta_{1j}\sin\alpha_{1j}\sin\gamma_{1j}$
$C_9 = -2\cos\alpha_{1j}\sin\alpha_{1j}\sin^2\beta_{1j}$
$C_{10} = -2\cos^2\beta_{1j}$
$C_{11} = -2\cos^2\alpha_{1j}\sin^2\beta_{1j}$
$C_{12} = -2\sin^2\alpha_{1j}\sin^2\beta_{1j}$
$C_{13} = \cos^2\gamma_{1j}\sin^2\beta_{1j}$
$C_{14} = \sin^2\beta_{1j}\sin^2\gamma_{1j}$
$C_{21} = C_3 + (1+\eta)C_2C_4 - (1-\eta)C_1C_5$
$C_{22} = C_6 + (1+\eta)C_2C_8 - (1-\eta)C_1C_7$
$C_{23} = C_9 + (1+\eta)C_5C_7 + (1-\eta)C_4C_8$
$C_{24} = C_{10} + (1+\eta)C_{14} + (1-\eta)C_{13}$
$C_{25} = C_{11} + (1+\eta)C_4^2 + (1-\eta)C_5^2$
$C_{26} = C_{12} + (1+\eta)C_8^2 + (1-\eta)C_7^2.$

DESCRIPTION OF THE IN-PLANE REORIENTATION COMBINED WITH THE
OUT-OF-PLANE REORIENTATION OF THE GUEST BENZENE MOLECULE

A reference frame was set as shown in Figure 2 to describe the molecular motion. Twelve deuterium sites are generated by the in-plane 6-site reorientational motion combined with out-of-plane 2-site reorientation on the reference frame. Due to the space group of the crystal the two benzene rings are equivalent, so that the population of each deuterium is also equivalent. The deuteriums at sites 2 and 8 occupy the same position, but the directions of their PAS are different, corresponding to the slant of each benzene ring. The deuteriums at sites 5 and 11 are in the same situation. The molecular motion was considered as jumps among the twelve deuterium sites. In this case, a deuterium is able to jump to its adjacent sites on the same benzene ring and to the opposite site on the other benzene ring. For example, the deuterium at site 1 jumps to sites 2 and 6 with jump frequency of k_i, and site 7 with that of k_0.

Acknowledgments

References

1. B.G. Silbernagel, A.R. Garcia, J.M. Newsam and R. Hulme: *J. Phys. Chem.* **93**, 6506 (1989).
2. S. Nishikiori, C.I. Ratcliffe and J.A. Ripmeester: *J. Phys. Chem.* **95**, 1589 (1991).
3. C-H. Kim, T. Soma, S. Nishikiori and T. Iwamoto: *Chem. Lett.* 89 (1996).

4. K. Ochiai, Y. Mazaki, S. Nishikiori, K. Kobayashi and N. Hayashi: *J. Chem. Soc. Perkin Trans. 2*, 1139 (1996).
5. J.H. Ok, R.R. Vold, R.L. Vold and M.C. Etter: *J. Phys. Chem.* **93**, 7618 (1989).
6. G.A. Facey, C.I. Ratcliffe and J.A. Ripmeester: *J. Phys. Chem.* **99**, 12249 (1995).
7. T. Soma and T. Iwamoto: *J. Incl. Phenom.* in press.
8. I. Solomon: *Phys. Rev.* **110**, 61 (1958).
9. J.H. Davis, K.R. Jeffrey, M. Bloom, M.I. Valic and T.P. Higgs: *Chem. Phys. Lett.* **42**, 390 (1976).
10. H.W. Spiess and H. Sillescu: *J. Magn. Reson.* **42**, 381 (1981).
11. A.J. Vega and Z. Luz: *J. Chem. Phys.* **86**, 1803 (1987).
12. M.S. Greenfield, A.D. Ronemus, R.L. Vold, R.R. Vold, P.D. Ellis and T.E. Raidy: *J. Magn. Reson.* **72**, 89 (1987).
13. R.J. Wittebort, E.T. Olejniczak and R.G. Griffin: *J. Chem. Phys.* **86**, 5411 (1987).
14. A.E. Miev, K.D.M. Harris and F. Guillaume: *J. Phys. Chem.* **99**, 1156 (1995), and references therein.
15. E. Meirovitch, I. Belsky and S. Vega: *J Phys. Chem.* **88**, 1522 (1984).